

Comparative Magnetic Study of Electrochemically and Chemically Delithiated $\text{Li}_x\text{Mn}_2\text{O}_4$ and Li_xNiO_2

Kazuhiko Mukai* and Jun Sugiyama

Toyota Central Research and Development Laboratories, Inc., 41-1 Yokomichi, Nagakute, Aichi-gun, Aichi 480-1192

(Received June 22, 2009; CL-090582; E-mail: e1089@mosk.tytlabs.co.jp)

The magnetic nature of almost fully delithiated $\text{Li}_x\text{Mn}_2\text{O}_4$ and Li_xNiO_2 samples, which were prepared by both an electrochemical (EC-) and chemical (C-) reaction, has been investigated by dc-susceptibility measurements. The Curie–Weiss parameters for C- $\text{Li}_{0.07}\text{Mn}_2\text{O}_4$ are almost identical to those for EC- $\text{Li}_{0.03}\text{Mn}_2\text{O}_4$. On the contrary, the effective magnetic moment for C- $\text{Li}_{0.01}\text{NiO}_2$ ($1.43 \mu_B$) is roughly twice that for EC- $\text{Li}_{0.05}\text{NiO}_2$ ($0.71 \mu_B$), suggesting that the Ni valence is not simply determined by the Li/Ni ratio for C- $\text{Li}_{0.01}\text{NiO}_2$.

Nonaqueous electrolytes are usually used in current lithium-ion batteries, while in principle still based on Hunter's report,¹ in which a fully delithiated $\text{Li}_x\text{Mn}_2\text{O}_4$, i.e., $\lambda\text{-MnO}_2$ is produced by digesting LiMn_2O_4 in an acid solution. Using a similar procedure, Arai et al.² prepared an almost fully delithiated Li_xNiO_2 sample with $x = 0.04$. However, chemically delithiated sample should be different from the electrochemically delithiated one, because the sample is partially dissolved in acid only for the chemical delithiation. Nevertheless, the nature of the electrochemically and chemically delithiated samples has not been fully investigated, despite the structural and compositional analyses.

We have thus measured magnetic susceptibility (χ) for almost fully delithiated $\text{Li}_x\text{Mn}_2\text{O}_4$ and Li_xNiO_2 samples, in order to clarify the difference between them, since the magnetism at high temperature (T) is very sensitive to the average oxidation state of the transition metal (Me) ions; more correctly, to the effective magnetic moment (μ_{eff}) of the Me ions. Here, both Mn ions in $\text{Li}_x\text{Mn}_2\text{O}_4$ and Ni ions in Li_xNiO_2 should be in a $4+$ state for the fully delithiated samples. Furthermore, it should be noted that the oxygen stacking sequence for $\text{Li}_x\text{Mn}_2\text{O}_4$ is maintained in a cubic close-packed (ccp) structure down to $x \approx 0$,¹ while that for Li_xNiO_2 partially changes from the ccp structure to a hexagonal close-packed (hcp) structure below $x \leq 0.04$.²

A polycrystalline sample of LiMn_2O_4 was prepared by a solid-state reaction technique using reagent grade Li_2CO_3 and electrolytic manganese dioxide (Mitsui Mining & Smelting Co., Ltd., Japan). Reaction mixture was heated at 900°C for 12 h in air and then cooled at 5°C min^{-1} . A powder sample of LiNiO_2 was synthesized by using reagent grade LiNO_3 and NiCO_3 . The reaction mixture was heated at 650°C in oxygen flow for 12 h. The obtained powder was crushed, pressed into a pellet again, and finally fired at 750°C in an oxygen flow for 12 h. The obtained powders were characterized by a power XRD (RINT-2200, Rigaku Co., Ltd., Japan) analysis and an electrochemical charge/discharge test. Almost fully delithiated $\text{Li}_x\text{Mn}_2\text{O}_4$ and Li_xNiO_2 samples were prepared by two different procedures: one was an electrochemical reaction (EC-) in a non-aqueous lithium cell and the other was a chemical reaction (C-) as previously reported.^{1,2} For EC, a Li-metal sheet was used as a counter electrode. The electrolyte was 1 M LiPF_6 dissolved in ethylene carbonate/diethyl carbonate (3/7 by v/v) solution.

For C, 3.6 g of LiMn_2O_4 powder (2 g of LiNiO_2 powder) was immersed in 100 mL of HNO_3 solution and stirred for 24 h at ambient T . The concentration of HNO_3 solution was 0.50 M for LiMn_2O_4 (1.0 M for LiNiO_2), in order to complete the reaction. The product was filtered and dried at 60°C (40°C for LiNiO_2) for 24 h. The composition of the samples was determined by an inductively coupled plasma-atomic emission spectrometer (ICP-AES, type CIROS 120, Rigaku Co., Ltd., Japan). χ was measured using a superconducting quantum interference device magnetometer (MPMS, Quantum Design) in the T range between 5 and 350 K under the magnetic field with $H = 10 \text{ kOe}$. The EC-samples were removed from the cells in an argon-filled glovebox just before the χ measurements.

The XRD analysis showed that the LiMn_2O_4 sample has a spinel structure with space group of $Fd\bar{3}m$, while the LiNiO_2 sample is identified as a layered structure with space group of $R\bar{3}m$. The lattice parameters are calculated as $a_c = 8.237 \text{ \AA}$ for LiMn_2O_4 and $a_h = 2.875$, $c_h = 14.203 \text{ \AA}$ for LiNiO_2 . Figure 1 shows the charge curves of (a) Li/ LiMn_2O_4 and (b) Li/ LiNiO_2 cells for the χ measurements. The cells were operated at a current density with 0.17 mA cm^{-2} for (a) and 0.057 mA cm^{-2} for (b). Here, the electrode for (a) consists of 88 wt % LiMn_2O_4 , 6 wt % conductive carbon, and 6 wt % binder, while that for (b) was made from 100 wt % LiNiO_2 . The charge curve for LiMn_2O_4 shows two distinct regions: the continuous change in the voltage vs. capacity below 4.1 V and flat operating voltage region at ca. 4.2 V. The charge curve for LiNiO_2 exhibits three plateaus around 3.6, 4.0, and 4.2 V. The electrochemical properties for the present samples are in good agreement with previously reported results for nearly stoichiometric LiMn_2O_4 ³ and LiNiO_2 .⁴

Figure 2 shows the T dependence of (a) χ and (b) χ^{-1} for the LiMn_2O_4 , EC- $\text{Li}_{0.03}\text{Mn}_2\text{O}_4$, and C- $\text{Li}_{0.07}\text{Mn}_2\text{O}_4$ samples. The $\chi(T)$ curve for C- $\text{Li}_{0.07}\text{Mn}_2\text{O}_4$ is almost identical to that for EC- $\text{Li}_{0.03}\text{Mn}_2\text{O}_4$. As T decreases from 350 K, the $\chi^{-1}(T)$ curves for all the samples exhibit a Curie–Weiss paramagnetic behavior down to ca. 200 K, except for a small cusp at ca. 285 K ($=T_{\text{JT}}$) for

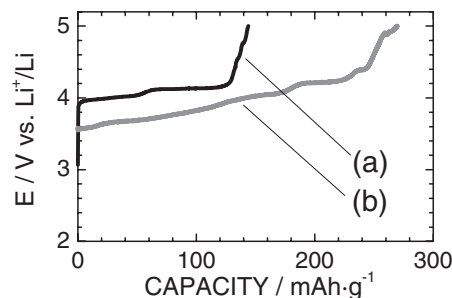


Figure 1. Charge curves for (a) Li/ LiMn_2O_4 and (b) Li/ LiNiO_2 cells for the χ measurements. The cells were operated at a current density with 0.17 mA cm^{-2} for (a) and 0.057 mA cm^{-2} for (b). The open circuit voltage before the χ measurements was 4.346 V for (a) and 4.317 V for (b).

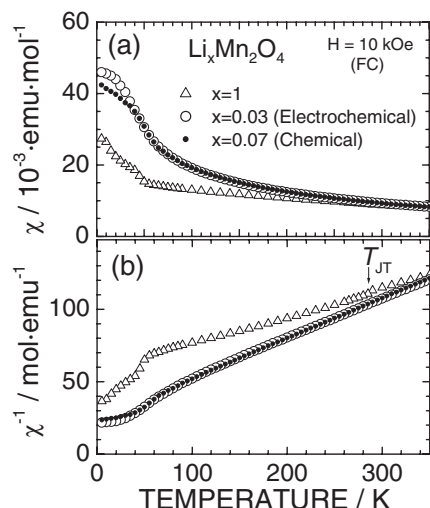


Figure 2. T dependence of (a) χ and (b) χ^{-1} for the LiMn_2O_4 , EC- $\text{Li}_{0.03}\text{Mn}_2\text{O}_4$, and C- $\text{Li}_{0.07}\text{Mn}_2\text{O}_4$ samples. The EC- $\text{Li}_{0.03}\text{Mn}_2\text{O}_4$ and C- $\text{Li}_{0.07}\text{Mn}_2\text{O}_4$ samples were prepared by electrochemical and chemical reaction, respectively.

Table 1. The Curie–Weiss parameters for $\text{Li}_x\text{Mn}_2\text{O}_4$ and Li_xNiO_2 ^a

| Sample | $\mu_{\text{eff}}/\mu_{\text{B}}$ | $\Theta_{\text{p}}/\text{K}$ | $\chi_0^b \times 10^{-3} / \text{emu mol}^{-1}$ | $\mu_{\text{eff}}^{\text{pre}} / \mu_{\text{B}}$ | $\delta\mu_{\text{eff}}^{\text{pre}} / \mu_{\text{B}}$ |
|---------------------------------------------|-----------------------------------|------------------------------|-------------------------------------------------|--------------------------------------------------|--------------------------------------------------------|
| LiMn_2O_4 | 4.40(2) | −260(5) | 0 | 4.42 | 0.005 |
| EC- $\text{Li}_{0.03}\text{Mn}_2\text{O}_4$ | 3.80(2) | −89(2) | 0 | 3.89 | 0.006 |
| C- $\text{Li}_{0.07}\text{Mn}_2\text{O}_4$ | 3.85(2) | −98(3) | 0 | 3.91 | 0.006 |
| LiNiO_2 | 2.03(1) | 49(1) | 0.003(6) | 1.73 | 0.009 |
| EC- $\text{Li}_{0.05}\text{NiO}_2$ | 0.71(1) | 24(2) | 0.08(1) | 0.39 | 0.04 |
| C- $\text{Li}_{0.01}\text{NiO}_2$ | 1.43(9) | 46(2) | 0.08(2) | 0.17 | 0.17 |

^a μ_{eff} and Θ_{p} for $\text{Li}_x\text{Mn}_2\text{O}_4$ and Li_xNiO_2 were obtained by fitting the $\chi(T)$ curves in the T range between 200 and 350 K with eq 1. ^bSince the $\chi^{-1}(T)$ curves for Li_xNiO_2 show a convex curve probably due to ferrimagnetism, we used T -independent susceptibility (χ_0) for the fitting in the T range between 200 and 350 K. ^cConsidering the analytical error in the ICP-AES analysis ($\delta x = 0.01$), $\delta\mu_{\text{eff}}^{\text{pre}}$'s were calculated.

LiMn_2O_4 . The cusp is attributed to the structural phase transition due to a cooperative Jahn–Teller (JT) transition of the Mn^{3+} ions.⁵ For a paramagnetic state, the Curie–Weiss law is written as:

$$\chi = \frac{N\mu_{\text{eff}}^2}{3k_{\text{B}}(T - \Theta_{\text{p}})} + \chi_0 \quad (1)$$

where N is the number density of the Mn (Ni) ions, μ_{eff} is the effective magnetic moment of the Mn (Ni) ions, k_{B} is the Boltzmann constant, T is the absolute temperature, Θ_{p} is the paramagnetic Curie T , and χ_0 is the T -independent susceptibility. Using eq 1 in the T range between 200 and 350 K, we obtain the values of μ_{eff} and Θ_{p} for the $\text{Li}_x\text{Mn}_2\text{O}_4$ samples as shown in Table 1. Here, the predicted $\mu_{\text{eff}}^{\text{pre}}$ was calculated under the assumption that Mn^{3+} ions are in the high-spin state with $t_{2g}^3e_g^1$ ($S = 2$), Mn^{4+} ions with t_{2g}^3 ($S = 3/2$), and the gyromagnetic constant $g = 2$. Since the obtained μ_{eff} 's for both EC- $\text{Li}_{0.03}\text{Mn}_2\text{O}_4$ and C- $\text{Li}_{0.07}\text{Mn}_2\text{O}_4$ are very close to $\mu_{\text{eff}}^{\text{pre}}$, μ_{eff} 's for both samples are well explained by the Mn valence estimated by the Li/Mn ratio.

Figure 3 shows the T dependence of (a) χ and (b) χ^{-1} for the LiNiO_2 , EC- $\text{Li}_{0.05}\text{NiO}_2$, and C- $\text{Li}_{0.01}\text{NiO}_2$ samples. The $\chi(T)$ curve for LiNiO_2 exhibits a rapid increase below ca. 100 K, indicating the presence of the localized moments of Ni ions. The

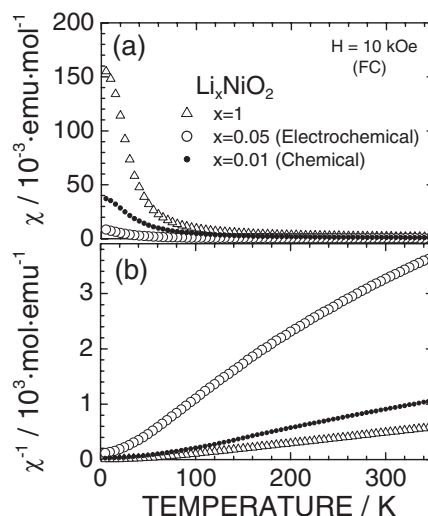


Figure 3. T dependence of (a) χ and (b) χ^{-1} for the LiNiO_2 , EC- $\text{Li}_{0.05}\text{NiO}_2$, and C- $\text{Li}_{0.01}\text{NiO}_2$ samples. The EC- $\text{Li}_{0.05}\text{NiO}_2$ and C- $\text{Li}_{0.01}\text{NiO}_2$ samples were prepared by electrochemical and chemical reaction, respectively.

magnitude of χ for EC- $\text{Li}_{0.05}\text{NiO}_2$ is significantly small compared to that for LiNiO_2 . Moreover, μ_{eff} for LiNiO_2 (EC- $\text{Li}_{0.05}\text{NiO}_2$) is larger by $0.3 \mu_{\text{B}}$ ($0.32 \mu_{\text{B}}$) than $\mu_{\text{eff}}^{\text{pre}}$, which are calculated by the assumption that both Ni^{3+} and Ni^{4+} ions are in the low-spin state with $t_{2g}^6e_g^1$ ($S = 1/2$) and t_{2g}^6 ($S = 0$), and $g = 2$. This suggests that g is larger than 2 probably due to a distortion of the NiO_6 octahedra. Anyway, the decrease in μ_{eff} with decreasing x means that the magnetic Ni^{3+} ions are oxidized to the nonmagnetic Ni^{4+} ions by the electrochemical reaction. The magnitude of χ for C- $\text{Li}_{0.01}\text{NiO}_2$ is larger than that for EC- $\text{Li}_{0.05}\text{NiO}_2$ in the whole T range measured. Also, the estimated μ_{eff} for C- $\text{Li}_{0.01}\text{NiO}_2$ ($1.43 \mu_{\text{B}}$) is roughly twice that for EC- $\text{Li}_{0.05}\text{NiO}_2$ ($0.71 \mu_{\text{B}}$). This indicates that the average Ni valence is not simply determined by the Li/Ni ratio for C- $\text{Li}_{0.01}\text{NiO}_2$, even if we consider the enhancement of g -factor and/or analytical error in the Li content of the ICP-AES analysis ($\delta x = 0.01$).

In conclusion, the magnetism for C- $\text{Li}_{0.01}\text{NiO}_2$ is rather different from that for EC- $\text{Li}_{0.05}\text{NiO}_2$. This implies that EC-samples are different from C-samples only for layered materials with the (partially) hcp structure. A series of nickel (oxy)hydroxide, which are electrode materials for Ni-MH cells, are also in the hcp structure. Therefore, the presence of H^+ ions would be responsible for the difference. More detailed structural and magnetic analyses for Li_xNiO_2 are in progress and will be reported elsewhere.

This work is partially supported by Grant-in-Aid for Scientific Research (B), 1934107, MEXT, Japan.

References

- 1 J. C. Hunter, *J. Solid State Chem.* **1981**, 39, 142.
- 2 H. Arai, M. Tsuda, K. Saito, M. Hayashi, K. Takei, Y. Sakurai, *J. Solid State Chem.* **2002**, 163, 340.
- 3 T. Ohzuku, M. Kitagawa, T. Hirai, *J. Electrochem. Soc.* **1990**, 137, 769.
- 4 T. Ohzuku, A. Ueda, M. Nagayama, *J. Electrochem. Soc.* **1993**, 140, 1862.
- 5 J. Sugiyama, T. Hioki, S. Noda, M. Kontani, *J. Phys. Soc. Jpn.* **1997**, 66, 1187.